On the Dual-Tree Complex Wavelet Packet and M-Band Transforms

İlker Bayram, *Student Member, IEEE,* and Ivan W. Selesnick, *Member, IEEE*

Abstract

The 2-band discrete wavelet transform (DWT) provides an octave-band analysis in the frequency domain, but this might not be 'optimal' for a given signal. The discrete wavelet packet transform (DWPT) provides a dictionary of bases over which one can search for an optimal representation (without constraining the analysis to an octave-band one) for the signal at hand. However, it is well known that both the DWT and the DWPT are shift-varying. Also, when these transforms are extended to 2-D and higher dimensions using tensor products, they do not provide a geometrically oriented analysis. The dual-tree complex wavelet transform (DT-$\mathbb{C}$WT), introduced by Kingsbury, is approximately shift-invariant and provides directional analysis in 2-D and higher dimensions. In this paper, we propose a method to implement a dual-tree complex wavelet packet transform (DT-$\mathbb{C}$WPT), extending the DT-$\mathbb{C}$WT as the DWPT extends the DWT. To find the best complex wavelet packet frame for a given signal, we adapt the basis selection algorithm by Coifman and Wickerhauser, providing a solution to the basis selection problem for the DT-$\mathbb{C}$WPT. Lastly, we show how to extend the 2-band DT-$\mathbb{C}$WT to an M-band DT-$\mathbb{C}$WT (provided that $M = 2^b$) using the same method.

Index Terms

Dual-tree complex wavelet transform, wavelet packet.

I. INTRODUCTION

The discrete wavelet transform (DWT), obtained by iterating a perfect reconstruction (PR) filter bank (FB) on its low-pass output, decomposes a discrete-time signal according to an octave-band frequency

decomposition as illustrated in the first panel of Figure 1. However, as is well known, the DWT is far from being shift-invariant and does not provide a geometrically oriented decomposition in multiple dimensions (perpendicular orientations are mixed in a single subband). One alternative to the DWT that does have those properties is the dual-tree complex wavelet transform (DT-$\mathbb{C}$WT) introduced by Kingsbury [10], [12], [20]. In addition to the wavelet FB utilized by the DWT, the DT-$\mathbb{C}$WT utilizes a second wavelet FB, designed according to a certain criterion. Specifically, the second wavelet FB is designed so that its impulse responses are approximately the discrete Hilbert transforms of those of the first wavelet FB. Then, regarding the first FB as the real part and the second FB as the imaginary part of a complex transform, the frequency analysis shown in the second panel of Figure 1 is achieved. That the frequency response of each channel is approximately analytic is important for the DT-$\mathbb{C}$WT to posses its desirable properties.

For a specific signal (or set of signals), the frequency decomposition provided by the DWT (and DT-$\mathbb{C}$WT) might not be optimal. To find a more suitable decomposition, algorithms have been proposed to find the "best-basis" from a structured dictionary of bases via suitable optimization [14]. For example, a best-basis algorithm that finds a sparse representation by minimizing the transform-domain entropy is proposed in [5], and an algorithm that finds the best basis in a rate-distortion sense is proposed in [17]. One way to generalize the DWT so as to generate a structured dictionary of bases is given by the discrete wavelet packet transform (DWPT). The (full) DWPT, obtained by iterating a PR FB on both its low-pass and high-pass output, provides a frequency-domain analysis as illustrated in the third panel of Figure 1 (for a 4-level DWPT). However, like the DWT, the DWPT is also shift-variant and mixes perpendicular orientations in multiple dimensions.

In this paper, we address the problem of constructing a complex (approximately analytic) version of the DWPT by utilizing the dual-tree approach. Like the DT-$\mathbb{C}$WT, such a dual-tree complex wavelet packet transform (DT-$\mathbb{C}$WPT) should be approximately shift-invariant and, in multiple dimensions, geometrically oriented. The most straight-forward way to generate a complex dual-tree form of the DWPT is to extend each of the two DWTs used to construct the DT-$\mathbb{C}$WT into packets themselves using the same set filters, an approach described previously in [6]–[8], [24][1]. However, for several subbands in this construction, significant energy leaks into the negative frequency band as illustrated in the fourth panel of Figure 1.

---

[1]Specifically, this construction is described as follows. Given a DT-$\mathbb{C}$WT with dual-tree filters $h_i(n)$ for the first FB and $h_i'(n)$ for the second FB, where $i \in \{0, 1\}$, one iterates the high-pass branches in the first FB using $h_i(n)$ and the high-pass branches in the second FB using $h_i'(n)$.

Those subbands are far from being approximately analytic. Unfortunately, as a result, this construction does not fully possess the desired properties of a DT-$\mathbb{C}$WPT.

In the following, we describe the development of a new DT-$\mathbb{C}$WPT that avoids the shortfall of the straightforward construction. In particular, given a DT-$\mathbb{C}$WT, it will be shown how to obtain a DT-$\mathbb{C}$WPT with approximately analytic subband responses. This (approximately analytic) DT-$\mathbb{C}$WPT provides the desired frequency analysis as illustrated in the fifth panel of Figure 1. Like the DT-$\mathbb{C}$WT, this DT-$\mathbb{C}$WPT is approximately shift-invariant and provides a geometrically oriented signal analysis in multiple dimensions. Like the DWPT, the new DT-$\mathbb{C}$WPT provides a structured dictionary of frames. Algorithms for best complex wavelet packet frames can be obtained by modifying existing best-basis algorithms. It will be demonstrated in the following that the best frame computed using the DT-$\mathbb{C}$WPT is less sensitive to signal translation than the best basis computed using the DWPT.

The DT-$\mathbb{C}$WT, which was originally developed using two 2-band DWTs was extended to M-band DWTs recently in [2], and used for image processing in [3]. The M-band DT-$\mathbb{C}$WT in [2], [3] employs two M-band discrete wavelet transforms where the wavelets associated with the two transforms form Hilbert transform pairs. For $M = 2^b$, we also describe a simple construction of an M-band DT-$\mathbb{C}$WT, based on the DT-$\mathbb{C}$WPT. We reported a prior version of these results in [1].

Notation and Definitions

Sequences are represented by lower case letters as in, $c(n)$. The z-transforms of the sequences are represented by capital letters, as $C(z)$, possibly evaluated on the unit circle, as $C(e^{j\omega})$. When we refer to the frequency response of a time-varying linear system like the one shown on the top panel of Figure 2, we mean the frequency response of the filter in the equivalent structure shown on the bottom panel. $\mathcal{H}\{.\}$ refers to either the continuous or the discrete-time Hilbert transform operator. Which one is used should be clear from the context.

II. PROPERTIES OF THE DT-$\mathbb{C}$WT

The DT-$\mathbb{C}$WT consists of two wavelet transforms operating in parallel on an input signal as illustrated in Figure 3. We denote the wavelet associated with the first wavelet FB as $\psi(t)$ and the wavelet associated with the second FB as $\psi'(t)$. The wavelet $\psi(t)$ is defined by

$$\psi(t) = \sqrt{2} \sum_n h_1(n)\, \phi(2t - n),$$

where

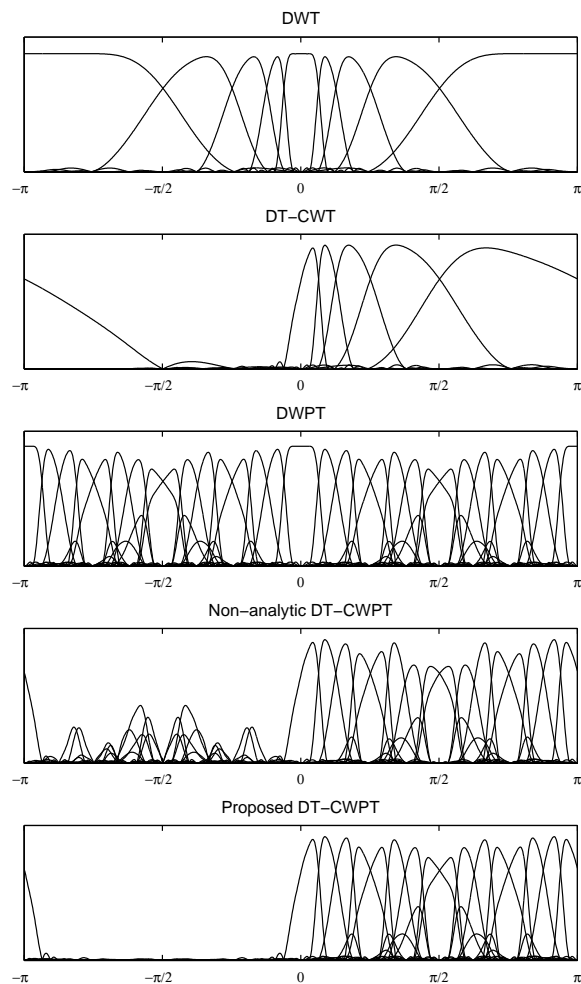$$\phi(t) = \sqrt{2} \sum_n h_0(n)\, \phi(2t - n).$$

Fig. 1. Frequency domain analysis (see 'Notation and Definitions') of DWT, DT-ℂWT, DWPT, the DT-ℂWPT developed in [6]–[8], [24] and the proposed DT-ℂWPT. Each figure is produced using the same set of Q-shift filters [13] of length 14. The proposed complex wavelet packet transform provides the desired approximately analytic frequency decomposition.
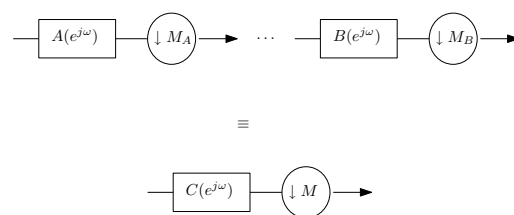

Fig. 2. The iterated filtering and downsampling operation is equivalent to a system expressed as a single filtering followed by a donwsampling operation.
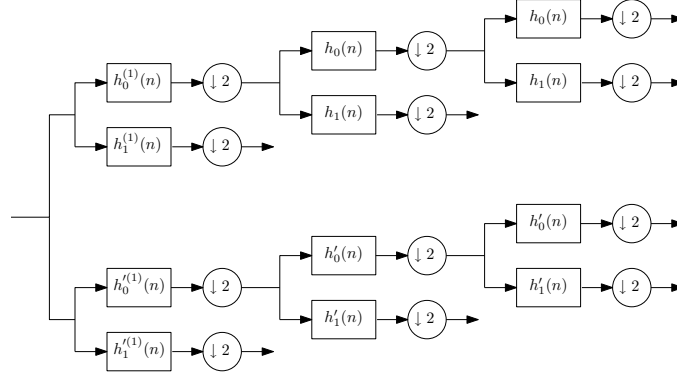
Fig. 3. The DT-ℂWT is implemented using two wavelet filter banks operating in parallel.

The second wavelet, $\psi'(t)$, is defined similarly in terms of $\{h'_0(n), h'_1(n)\}$.

For the ideal DT-ℂWT, the second wavelet, $\psi'(t)$, is the Hilbert transform of the first wavelet, $\psi(t)$,

$$\psi'(t) = \mathcal{H}\{\psi(t)\}. \tag{1}$$

It was shown in [18] that if the low-pass filter $h'_0(n)$ is equal to the half-sample delayed version of $h_0(n)$ (to be formalized below), then the wavelets generated by the DT-ℂWT satisfy (1) as desired. This condition was later proved ([16] [25]) to be necessary as well. To construct the DT-ℂWPT (the packet form of the DT-ℂWT), it is also important to use the consequential relationship among the high-pass filters, $h_1(n)$ and $h'_1(n)$. We assume that $\{h_0(n), h_1(n)\}$ form an FIR conjugate quadrature filter (CQF) pair, as does $\{h'_0(n), h'_1(n)\}$.

Suppose we are given wavelets, $\psi(t)$ and $\psi'(t)$, satisfying (1). It was shown in [25], that if each wavelet is orthogonal to its integer translates, then the Hilbert relation (1) is satisfied if and only if, [2]

$$H'_0(e^{j\omega}) = e^{-j\,0.5\,\omega}\,H_0(e^{j\,\omega}) \quad \text{for } |\omega| < \pi. \tag{2}$$

Recall that for an orthonormal wavelet basis, the low-pass and high-pass filters are related as $H_1(e^{j\omega}) = -e^{-j\,d\omega}\,H_0^*(e^{j(\omega-\pi)})$ (equivalently $h_1(n) = (-1)^n\,h_0(d-n)$) where '$d$' is an odd integer. Hence, it

[2] It should be noted that the most general condition is actually $H'_0(e^{j\omega}) = e^{-j((2m+1)\omega/2)}H_0(e^{j\omega})$ for $|\omega| < \pi$ and some $m \in \mathbb{Z}$ [3]. Only $m = 0$ is considered in [25], but it can be seen, following the treatment given there, that the condition is valid when m is a non-zero integer as well. However, it can be shown that m values other than 0 and -1 give poor directionality when used for the implementation of a 2-dimensional DT-ℂWT. Noting that one can modify m to any desired integer value by shifting the filters accordingly and possibly changing the roles of the trees, we concentrate, without loss of generality, on the $m = 0$ case.
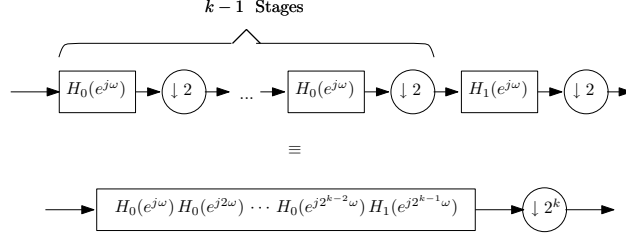
Fig. 4. Response of the kth stage high-pass branch and its equivalent.

follows from (2) that for the ideal DT-$\mathbb{C}$WT, the high-pass filters satisfy

$$H_1'(e^{j\omega}) = -j\,\text{sgn}(\omega)\,e^{j\,0.5\,\omega}\,H_1(e^{j\omega}) \quad \text{for } |\omega| < \pi, \tag{3}$$

where 'sgn' is the signum function.

The development of the discrete implementation of the DT-$\mathbb{C}$WPT in Section III builds upon a close analysis of the filter banks used. As described in [20], for the correct implementation of the DT-$\mathbb{C}$WT, the first stage of FB requires special attention. (Otherwise, the frequency responses of the first several stages will be far from analytic.) In the following, we explain why the first stage of the DT-$\mathbb{C}$WT must be different from the following stages, by giving an explicit expression for the frequency response at each stage of the transform. By asking that the frequency response of the second wavelet FB at stage k be the Hilbert transform of that of the first wavelet FB, for every stage $k \geq 1$, we obtain the condition required of the first stage. This explanation, for why the first stage must be different from the following stages, is quite different from the explanation in [20].

Consider the kth stage of the first FB terminated with $H_1(e^{j\omega})$ as illustrated in Figure 4. Denoting the equivalent response by $H^{(k)}(e^{j\omega})$ we can use the noble identities to write, for $k > 1$,

$$H^{(k)}(e^{j\omega}) = H_1(e^{j2^{k-1}\omega}) \prod_{m=0}^{k-2} H_0(e^{j2^m\omega}) \quad \text{for } |\omega| < \pi. \tag{4}$$

Suppose that the equivalent response of the second FB's corresponding branch, which is obtained by replacing H_i by H_i', is denoted by $H'^{(k)}(e^{j\omega})$. If we further define,

$$H^{(1)}(e^{j\omega}) = H_1(e^{j\omega}) \tag{5}$$

$$H'^{(1)}(e^{j\omega}) = H_1'(e^{j\omega}) \tag{6}$$

we have the following lemma.

Lemma 1: Given CQF pairs $\{h_0(n), h_1(n)\}$, $\{h_0'(n), h_1'(n)\}$ that satisfy (2), (3), it follows that, for all $k \geq 1$, $H'^{(k)}(e^{j\omega})$ and $H'^{(k)}(e^{j\omega})$ satisfy,

$$H'^{(k)}(e^{j\omega}) = -j\,\text{sgn}(\omega)\,e^{j0.5\omega}\,H^{(k)}(e^{j\omega}) \quad \text{for } |\omega| < \pi, \tag{7}$$

which is equivalent to,[3]

$$\frac{H'^{(k)}(e^{j\omega})}{H^{(k)}(e^{j\omega})} = \frac{H_1'(e^{j\omega})}{H_1(e^{j\omega})}$$

$$= -j\,\text{sgn}(\omega)e^{j0.5\omega} \quad \text{for } |\omega| < \pi. \tag{8}$$

Proof: See the appendix. ∎

Equation (7) may also be written as,

$$H'^{(k)}(e^{j\omega}) = -e^{j0.5\omega}\mathcal{H}\left\{H^{(k)}(e^{j\omega})\right\}.$$

Therefore, by delaying the input to the second wavelet FB by a half-sample (by multiplying its Fourier transform by $e^{-j0.5\omega}$), the frequency response of the first wavelet FB would be equal to the Hilbert transform of the frequency response of the second wavelet FB, for every stage $k \geq 1$, except for the low-pass band. That is the desired property of the discrete implementation of the DT-$\mathbb{C}$WT.[4] However, an ideal half-sample delay requires an infinite impulse response (IIR) system. If we accept a non-ideal half-sample delay system and ask for an invertible approximate half-sample delay system, then we could use a realizable all-pass system; that will also be IIR.

Instead of using a half-sample delay system, we now consider the case where the filters of the first stage are allowed to be different from the following stages, as illustrated in Figure 3. Denote by $h_i^{(1)}(n)$ and $h_i'^{(1)}(n)$ the filters in the first stage, as in Figure 3. Also, denoting the new k^{th} stage response of the first FB by $H_{\text{new}}^{(k)}(e^{j\omega})$ and that of the second FB by $H_{\text{new}}'^{(k)}(e^{j\omega})$, we have the following result as a corollary of Lemma 1.

Corollary 1: Suppose we are given CQF pairs $\{h_0(n), h_1(n)\}$, $\{h_0'(n), h_1'(n)\}$ that satisfy (2), (3). For $k > 1$,

$$H_{\text{new}}^{(k)}(e^{j\omega}) = \mathcal{H}\left\{H_{\text{new}}'^{(k)}(e^{j\omega})\right\}, \tag{9}$$

if and only if

$$h_0'^{(1)}(n) = h_0^{(1)}(n-1). \tag{10}$$

---

[3]We ignore the zeros on the unit circle.

[4] However, in [3], the authors, following a different interpretation of the dual-tree transform, reach another set of prefilters. The prefilters we present here are the same as in [20].

Proof: See the appendix. ∎

Note that any PR FB can be used for the first stage; it does not need to be one designed specifically for the DT-$\mathbb{C}$WT.[5] If the first stage of the DT-$\mathbb{C}$WT is chosen in this way and if the remaining stages satisfy (2) exactly, then the transform will be exactly analytic at every stage except the first stage. (If the remaining stages satisfy (2) approximately, then the DT-$\mathbb{C}$WT will be approximately analytic at every stage except the first stage.)

III. The Dual-Tree Complex Wavelet Packet Transform

To construct a packet form of the DT-$\mathbb{C}$WT each of the subbands should be repeatedly decomposed using low-pass/high-pass PR FBs. The PR FBs should be chosen so that the response of each branch of the second wavelet packet FB is the discrete Hilbert transform of the corresponding branch of the first wavelet packet FB. Then each subband of the the DT-$\mathbb{C}$WPT will be analytic. This requirement can be fulfilled with a simple rule which is derived below.

First, note that if a given filter $g(n)$ is the discrete Hilbert transform of some other filter $h(n)$, that is,

$$G(e^{j\omega}) = j \operatorname{sgn}(\omega) H(e^{j\omega}) \quad \text{for } |\omega| < \pi, \tag{11}$$

then when $g(n)$ is convolved with some sequence $c(n)$, we have,

$$G(e^{j\omega}) C(e^{j\omega}) = j \operatorname{sgn}(\omega) H(e^{j\omega}) C(e^{j\omega}) \quad \text{for } |\omega| < \pi. \tag{12}$$

As shown by this equation, if $h(n)$ and $g(n)$ is a discrete Hilbert transform pair, then $g(n) * c(n)$ and $h(n) * c(n)$ is also a discrete Hilbert transform pair. The preceding discussion is basically a consequence of the fact [15] that the discrete Hilbert Transform may be regarded as a linear time-invariant (LTI) system.

Now turning back to the DT-$\mathbb{C}$WT, suppose we decompose the kth stage highpass subband of the DT-$\mathbb{C}$WT using some 2-channel PR FBs as shown in Figure 5. We want to determine conditions on the filters $f_i(n)$, $f_i'(n)$ such that the resulting DT-$\mathbb{C}$WPT is analytic. From Section II, we know that $H^{(k)}(e^{j\omega}) = \mathcal{H}\left\{H'^{(k)}(e^{j\omega})\right\}$. Considering the equivalent structures provided, it follows from (11) and (12) that in order for the extended responses to be Hilbert transform pairs, that is, for

$$H^{(k)}(e^{j\omega}) F_i(e^{j2^k\omega}) = \mathcal{H}\left\{H'^{(k)}(e^{j\omega}) F_i'(e^{j2^k\omega})\right\}$$

---

[5] However, if orthonormality is desired in each FB of the DT-$\mathbb{C}$WT, then orthonormal FBs must be used for the first stage.
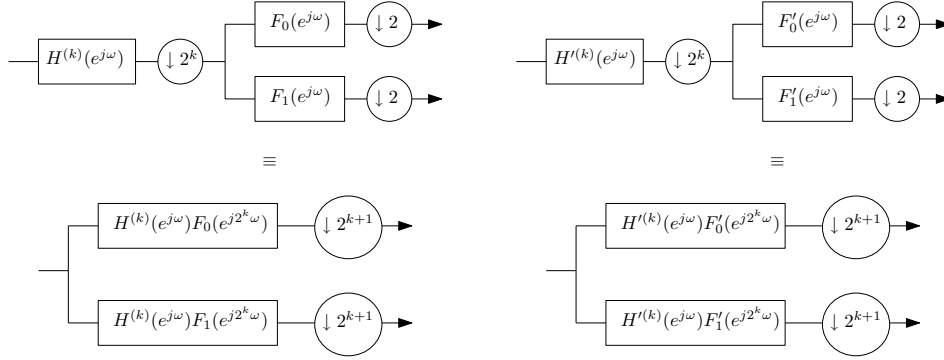
Fig. 5. On the left is the the kth subband of the first FB of the DT-$\mathbb{C}$WT further decomposed using filters $f_i(n)$ and the equivalent structure. On the right is the the kth stage of the second FB of the DT-$\mathbb{C}$WT extended using filters $f_i'(n)$ and the equivalent structure. If $H^{(k)} = \mathcal{H}\{H'^{(k)}\}$, then we need to set $f_i(n) = f_i'(n)$ to ensure that the extensions satisfy the Hilbert transform relationship as well.

to hold, it is necessary and sufficient that

$$f_i(n) = f_i'(n).$$

Therefore, we conclude that whatever PR FB is used to decompose the first FB of the DT-$\mathbb{C}$WT should also be used decompose the second (dual) FB — in order to preserve the Hilbert transform relationship already satisfied by those branches. The branches of the DT-$\mathbb{C}$WT that do not already satisfy the Hilbert transform property are the low-pass branch of the final stage and the high-pass branch of the first stage. Note that the low-pass branch of the final stage is not further decomposed. The high-pass branch of the first stage, that is, the filters $h_1^{(1)}(n)$ and $h_1'^{(1)}(n)$, satisfy $h_1'^{(1)}(n) = h_1^{(1)}(n-1)$, which is exactly the same relationship satisfied by the low-pass filters of the first stage, $h_0'^{(1)}(n) = h_0^{(1)}(n-1)$. Observing that the analysis carried out in the previous section for the DT-$\mathbb{C}$WT is dependent only on the relative delays, we conclude that the FB structure following the low-pass filters of the first stage should also follow the high-pass filters of the first stage. This procedure produces a DT-$\mathbb{C}$WPT consisting of two wavelet packet FBs operating in parallel, where some filters in the second wavelet packet FB are the same as those in the first wavelet packet FB. The first of these two wavelet packet FBs is illustrated in Figure 6, for a four-stage DT-$\mathbb{C}$WPT. The second wavelet packet FB is obtained by replacing the first stage filters $h_i^{(1)}(n)$ by $h_i^{(1)}(n-1)$ and by replacing $h_i(n)$ by $h_i'(n)$ for $i \in \{0,1\}$. The filters denoted by F_i in Figure 6 are unchanged in the second wavelet packet FB. The frequency responses of a four-stage DT-$\mathbb{C}$WPT are illustrated in the fifth panel of Figure 1 where it is clear that the responses are approximately analytic as desired.
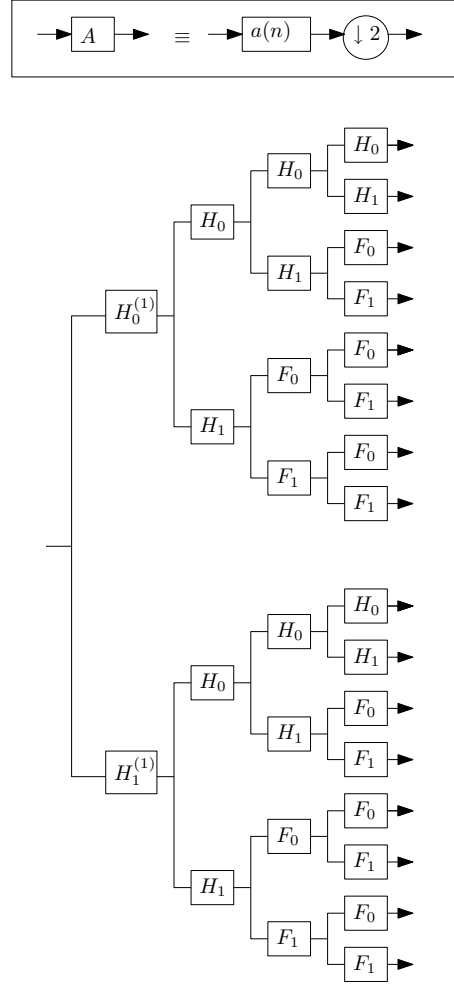
Fig. 6. The first wavelet packet FB of a four-stage DT-$\mathbb{C}$WPT. The second wavelet packet FB is obtained by replacing the first stage filters $h_i^{(1)}(n)$ by $h_i^{(1)}(n-1)$ and by replacing $h_i(n)$ by $h_i'(n)$ for $i \in \{0, 1\}$. The filters $f_i(n)$ are those that must be used in both FBs.

An important point about the transform described above is the choice of the extension filters $f_i(n)$. Notice that, preserving the Hilbert transform property, constrains only the transform so as to force the use of the same filter pair in both FBs. However, this does not place any restrictions on $f_i(n)$. Hence, the same criteria for the selection of a CQF pair to extend a regular DWT can be used for the selection of $f_i(n)$ (see [14] for instance). Filters with short support, frequency selectivity, or possessing a number of vanishing moments etc. can be used in accordance with the requirements of the application at hand.
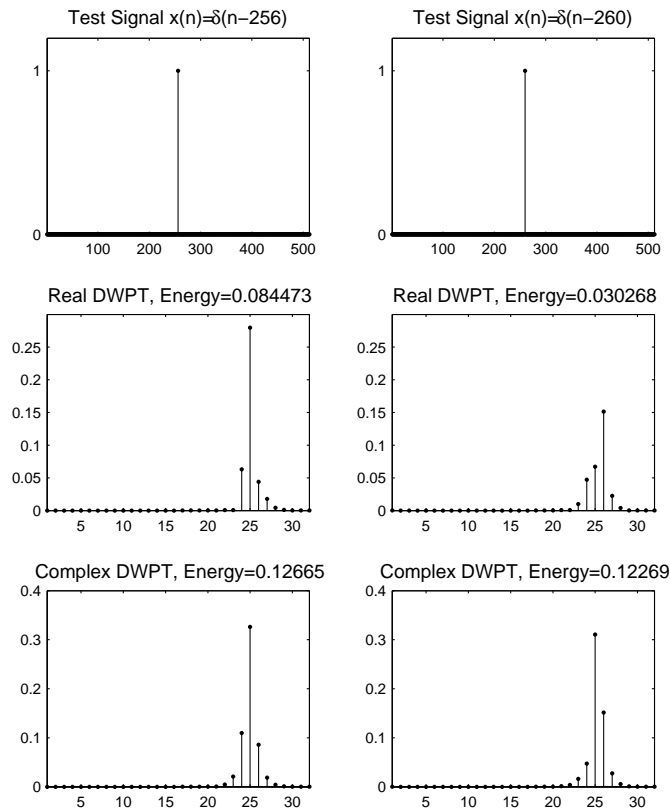
Fig. 7. The HLLH subband response to an impulse and translated impulse in the real DWPT and the DT-ℂWPT. The energy is approximately conserved for the DT-ℂWPT. Q-shift filters [13] of length 14 are used to produce this figure.

A. Approximate Shift-invariance of the DT-ℂWPT

As Figure 1 confirms, the developed DT-ℂWPT is approximately analytic. As a consequence, the multi-dimensional form of the transform will be geometrically oriented in two (and more) dimensions. In addition, in a sense, the transform is also approximately shift-invariant — the energy in each subband is approximately preserved if the input sequence is shifted by an arbitrary number of samples. Figure 7 illustrates this property. Because it is nearly shift-invariant, best-frame algorithms using the DT-ℂWPT are more robust to signal translation than best-basis algorithms using the real DWPT, as illustrated in Section III-B. This approximate shift-invariance property is due to the reduction in aliasing that takes place in the DT-ℂWPT compared to the real DWPT. The aliasing, caused by the down-samplers, is reduced in the DT-ℂWPT because the band-pass response of each branch is approximately analytic. We refer to Section 4 of [12] for a further explanation of this point.

We should note that DT-ℂWPT is not the only method for implementing an (approximately) shift-
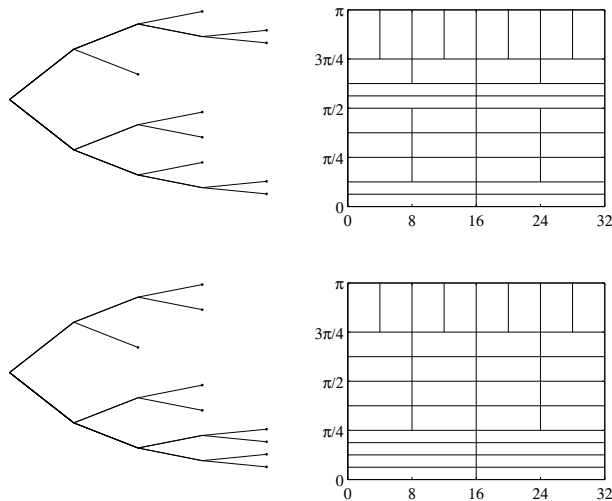
Fig. 8. Two bases derived from the DWPT and the corresponding ideal time-frequency tiling.

invariant wavelet packet decomposition. The orthonormal wavelet packet transform presented in [4] is exactly shift-invariant, also in the sense that the energy in each subband is invariant to translation of the input signal. However, for a given input signal, the algorithm of [4] attains shift-invariance by performing an exhaustive search over all of shifted wavelet packet bases to determine the 'best basis' (the one that provides a representation of the input signal minimizing a cost function). Thus, the transform is signal-dependent, and a disadvantage as noted in [4] is the complexity necessarily introduced by the search algorithm. In contrast, the DT-$\mathbb{C}$WPT is a fixed linear transform and necessitates only the design of DT-$\mathbb{C}$WT filters, on which a body of literature already exists [9], [11], [13], [19] (also see [20] for an overview).

B. Best Basis Selection

Allowing the iteration of the high-pass outputs as well as the low-pass outputs, the DWPT introduces a number of different structures (trees) to analyze the input (see Figure 8). Each tree yields a unique frequency decomposition of the input. Consequently, the same input is represented in a number of different bases, some representations being more sparse or compact than others. Thus, given an input, the search for a best basis among our collection of trees, in terms of expressing the input in the most compact way, makes sense in this setting. In the following, the search algorithm introduced in [5] for the DWPT, will be adapted to the DT-$\mathbb{C}$WPT.

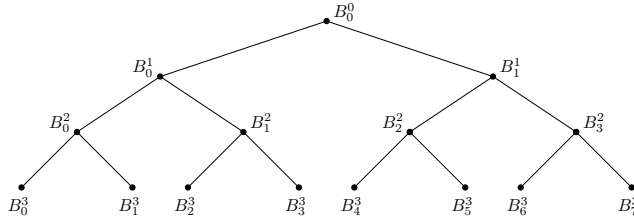The dynamic programming approach described by [5], [23] rests on the concept of an additive cost

Fig. 9. A tree introducing the notation for Algorithm 1.

function.

Definition 1: A cost function $\mathcal{C}(\cdot)$, mapping the sequences $\{x_i\}_{i=1}^N$ to real numbers, is additive if $\mathcal{C}(\{x_i\}) = \sum_i g(x_i)$ for some $g : \mathbb{R} \to \mathbb{R}$ and all $\{x_i\}_{i=1}^N$.

Following this definition, it is seen that instead of computing the cost function for each basis separately, the decision to keep the parent or its children at a particular point in the tree can be made locally. Notice that there are a number of different cost functions [23] that satisfy the above definition. The cost function we will consider in this paper is the Shannon entropy. To utilize the Shannon entropy, the underlying transform should be orthonormal and the input signal should be scaled so as to have unit energy. The algorithm to find the best tree is given as follows [23]:

Algorithm 1: Let B_k^n denote the kth vertex at the nth level for a tree, as shown in Figure 9. Let L be the highest level.

- *Scale the input so that it is a unit energy sequence.*
- *For each vertex B_k^n in the tree, compute the cost for the coefficients corresponding to that particular vertex. Let C_k^n denote the total cost at vertex B_k^n.*
- *For $n = L - 1$ to 1,*
    - *For $k = 0$ to $2^n - 1$,*
        - *If $C_k^n < C_{2k}^{n+1} + C_{2k+1}^{n+1}$, then prune the tree so that B_k^n is a leaf.*
        - *Otherwise, set $C_k^n := C_{2k}^{n+1} + C_{2k+1}^{n+1}$.*
    - *End Loop*
- *End Loop.*

We note at this point that even though the DT-$\mathbb{C}$WPT is not an orthonormal transform, it consists of two orthonormal transforms (which follow the same tree structure but use different filters at some vertices), provided that orthonormal FBs are used. Consequently, for each tree structure, regarding the coefficients from the first tree as the real part and the coefficients from the second tree as the imaginary
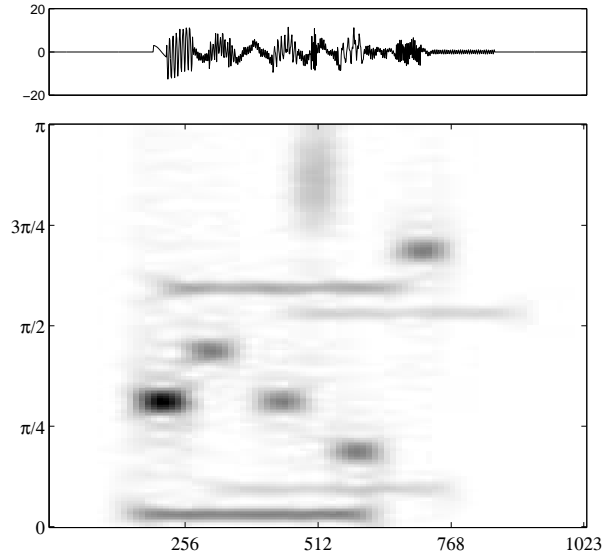
Fig. 10. The signal used in the 'best basis' selection experiment and its spectrogram. The length of the signal is 1024.

parts of a complex valued transform, the total energy of the DT-$\mathbb{C}$WPT coefficients is equal to two times the energy of the input function. Thus, if Step 1 in Algorithm 1 is modified so as to scale the input to have an input of energy 0.5, we see that we can use the algorithm to find the best basis for the DT-$\mathbb{C}$WPT as well.

For an input signal whose spectrogram is shown in Figure 10, using the Shannon entropy as the cost function, we found that the 'best basis' for both the DWPT and the DT-$\mathbb{C}$WPT is given by the upper panel in Figure 8. (Note the relation between the ideal frequency division provided by the best basis in Figure 8 and the spectrogram in Figure 10.) It is noted in [14] that due to the shift-variance of the DWPT, the best basis computed using Algorithm 1 might vary as the input signal is shifted. However, following the discussion in Section III-A regarding the approximate shift-invariance of the DT-$\mathbb{C}$WPT, we expect that the best basis for the DT-$\mathbb{C}$WPT be more stable compared to the best basis for the DWPT when the input signal is shifted. To test this, we circularly shifted the signal in Figure 10 (which is of length 1024) by k samples and computed the best basis for the DWPT and the DT-$\mathbb{C}$WPT as k is varied from 0 to 1023. It was seen that the best basis for the DT-$\mathbb{C}$WPT remains unchanged most of the time and that the best basis for the DWPT is more dependent on the amount of the shift. The results are tabulated in Figure 11. This example illustrates that the DT-$\mathbb{C}$WPT can be less sensitive to signal shifts than the real DWPT.
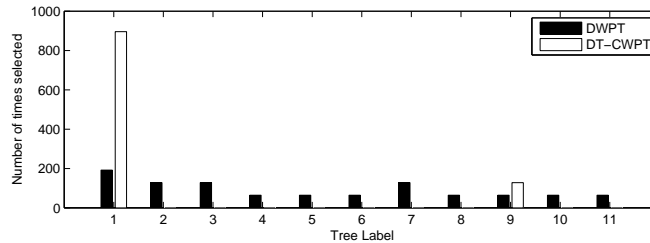
Fig. 11. Number of times each best basis is selected as the signal in Figure 10 is circularly shifted. The signal shift is varied from 0 to 1023. Eleven distinct bases are generated by the DWPT best basis algorithm as the test signal is circularly shifted. Tree 1 is the tree in the upper panel of Figure 8. Each tree provides a distinct frequency decomposition.
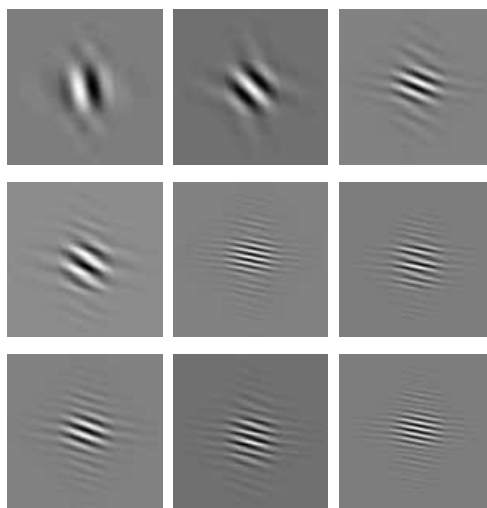

Fig. 12. Impulse responses of some of the filters used in T_{+-} at level-4.

C. 2-D Oriented Dual-Tree Wavelet Packet Transform

The DT-$\mathbb{C}$WPT may be extended to 2-D similar to the DT-$\mathbb{C}$WT [20]. We will briefly explain the 'real 2-D dual-tree wavelet packet transform'. The 'complex' case can be obtained similarly (see [20] for the definitions of 'real' and 'complex' 2-D dual-tree transforms).

First, the two transforms making up the dual-tree transforms are extended to 2-D similarly as the standard separable wavelet transform. Then, denoting the 2-D transform of the first tree by $\mathbf{T_1}$ and that of the dual-tree by $\mathbf{T_2}$, the 2-D real oriented 2-D dual-tree transform, is given by,

$$\mathbf{T_{2D}} = \begin{bmatrix} T_{+-} \\ T_{++} \end{bmatrix} := \frac{1}{2} \begin{bmatrix} \mathbf{I} & -\mathbf{I} \\ \mathbf{I} & \mathbf{I} \end{bmatrix} \begin{bmatrix} \mathbf{T_1} \\ \mathbf{T_2} \end{bmatrix}.$$

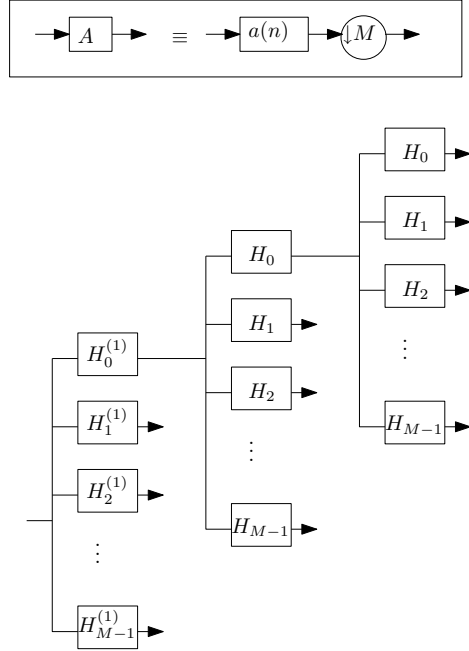Figure 12 illustrates the some of the impulse responses from T_{+-} employing the full-tree at level-4.

Fig. 13. The first filter bank of an M-band DT-$\mathbb{C}$WT. The filters of the first tree, are labeled as $h_0(n), h_1(n), \ldots, h_{M-1}(n)$, with an exception for the first stage. The second filter bank filters are denoted by primed labels, i.e. as $h_0'^{(1)}(n), \ldots, h_{M-1}'^{(1)}(n), h_0'(n), \ldots, h_{M-1}'(n)$.

IV. Implementing the M-Band DT-$\mathbb{C}$WT

The DT-$\mathbb{C}$WT discussed above employs two 2-band discrete transforms where one of the transforms is regarded as yielding the real part and the other yielding the imaginary part of the DT-$\mathbb{C}$WT. It is required that the frequency responses of the branches computing the real part and the imaginary part, form discrete Hilbert pairs. A generalization of this structure may be achieved by utilizing two M-band transforms (see Figure 13), with a similar interpretation in terms of real and imaginary responses, and the same discrete Hilbert transform relationship [2] (also see [3] for an application to image processing).

It can be shown for the 2-band case that, if the Hilbert transform relationship is required to be exact, the filters in both trees can not all be FIR [20]. This is the same for the M-band case. To overcome this problem, in [2], the authors approximate IIR filters using FIR filters by minimizing the $\mathbb{L}^2$ error of the frequency response and in [3] perform the filtering operations in the frequency domain. However, if attention is restricted to M-band DT-$\mathbb{C}$WTs with $M = 2^k$, one can employ 2-band DT-$\mathbb{C}$WPTs to realize these transforms. More specifically, a 2^k-band DT-$\mathbb{C}$WT can be obtained by pruning a full DT-
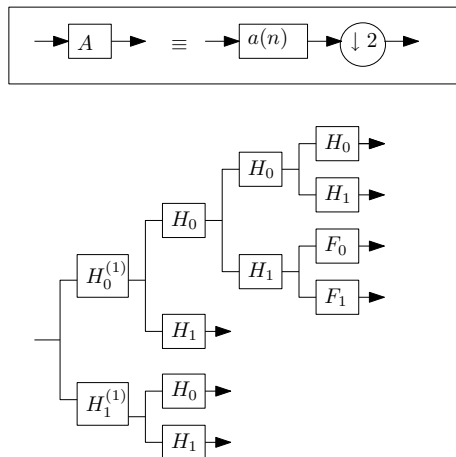
Fig. 14.   The first two stages of the first filter bank of the 4-band DT-ℂWT derived from the DT-ℂWPT. The second filter bank is obtained following the rule given in Figure 6.
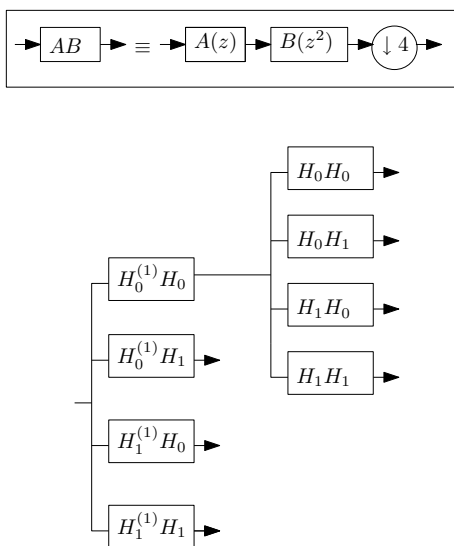

Fig. 15.   The 4-band filter bank equivalent to the filter bank given in Figure 14.

ℂWPT (see Figures 14,15). As a consequence, if we already have a DT-ℂWPT implemented using FIR filters (which thus satisfies the required properties approximately rather than exactly), we can obtain a reasonable approximation to the required discrete Hilbert property by using FIR filters. To appreciate this approximation, the sufficient phase condition is discussed in Section IV-A.

It is also instructive to consider Hilbert pairs of M-band wavelets and develop the M-band DT-ℂWT using these wavelet bases, as is done for the 2-band case. For convenience we consider the $M = 4$ case
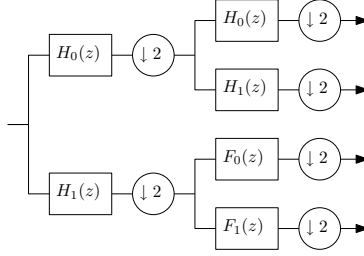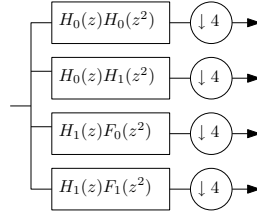
Fig. 16. A discrete wavelet packet transform.

Fig. 17. Equivalent of the filter bank in Figure 16.

in the following and obtain the 4-band DT-$\mathbb{C}$WT from a given 2-band DT-$\mathbb{C}$WT.

Suppose we are given a 2-channel orthonormal filter bank $\{h_0^{(2)}(n), h_1^{(2)}(n)\}$ and its associated scaling function $\phi^{(2)}(t)$ and wavelet $\psi^{(2)}(t)$, the Fourier transforms of which are defined by

$$\Phi^{(2)}(\omega) = \prod_{l=1}^{\infty} \left[\frac{1}{\sqrt{2}} H_0^{(2)} \left(\frac{\omega}{2^l} \right) \right],$$

$$\Psi^{(2)}(\omega) = \frac{1}{\sqrt{2}} H_1^{(2)} \left(\frac{\omega}{2} \right) \Phi^{(2)} \left(\frac{\omega}{2} \right).$$

Suppose we are also given a second 2-channel filter bank $\{h_0'^{(2)}(n), h_1'^{(2)}(n)\}$ and its associated scaling function $\phi'^{(2)}(t)$ and wavelet $\psi'^{(2)}(t)$, where $\psi'^{(2)}(t)$ is the Hilbert transform of $\psi^{(2)}(t)$, i.e.

$$\Psi'^{(2)}(\omega) = j\,\mathrm{sgn}(\omega)\Psi^{(2)}(\omega). \tag{13}$$

That is, we are given a 2-band 'dual-tree' complex wavelet transform where the complex wavelet $\psi^{(2)}(t)+ j\psi'^{(2)}(t)$ is analytic.

Now we would like to construct a 4-band complex wavelet transform. To that end, suppose that $\{f_0(n), f_1(n)\}$ is another 2-channel orthonormal filter bank. We can then obtain a 4-channel orthonormal filter bank, namely a discrete wavelet packet transform [14], as illustrated in Figure 16. Our aim is to construct a second wavelet packet transform so that the wavelets (associated with the two wavelet packet transforms) form Hilbert transform pairs. Using noble identities, it can be seen that the filter bank in

Figure 16 is equivalent to the filter bank in Figure 17. Now defining,

$$H_0^{(4)}(e^{j\omega}) := H_0^{(2)}(e^{j\omega})H_0^{(2)}(e^{j2\omega}),$$

$$H_1^{(4)}(e^{j\omega}) := H_0^{(2)}(e^{j\omega})H_1^{(2)}(e^{j2\omega}),$$

$$H_2^{(4)}(e^{j\omega}) := H_1^{(2)}(e^{j\omega})F_0(e^{j2\omega}),$$

$$H_3^{(4)}(e^{j\omega}) := H_1^{(2)}(e^{j\omega})F_1(e^{j2\omega}),$$

we can show, using the infinite product formulas for the M-band ($M = 4$) case [22],

$$\Phi^{(4)}(\omega) = \prod_{l=1}^{\infty}\left[\frac{1}{2}H_0^{(4)}\left(\frac{\omega}{4^l}\right)\right],$$

$$\Psi_k^{(4)}(\omega) = \frac{1}{2}H_k^{(4)}\left(\frac{\omega}{4}\right)\Phi^{(4)}\left(\frac{\omega}{4}\right), \quad k \in \{1, 2, 3\},$$

that the Fourier transforms of the scaling function and wavelets associated with this 4-channel filter bank can be written as,

$$\Phi^{(4)}(\omega) = \Phi^{(2)}(\omega),$$

$$\Psi_1^{(4)}(\omega) = \Psi^{(2)}(\omega),$$

$$\Psi_2^{(4)}(\omega) = \frac{1}{\sqrt{2}}F_0\left(\frac{\omega}{2}\right)\Psi^{(2)}\left(\frac{\omega}{2}\right), \tag{14}$$

$$\Psi_3^{(4)}(\omega) = \frac{1}{\sqrt{2}}F_1\left(\frac{\omega}{2}\right)\Psi^{(2)}\left(\frac{\omega}{2}\right).$$

Suppose now that we extend the second 2-channel filter bank similar to the first one as in Figure 16 but using a different 2-channel orthonormal filter bank $\{f_0'(n), f_1'(n)\}$. Then it follows as in (14) that,

$$\Phi'^{(4)}(\omega) = \Phi'^{(2)}(\omega),$$

$$\Psi_1'^{(4)}(\omega) = \Psi'^{(2)}(\omega),$$

$$\Psi_2'^{(4)}(\omega) = \frac{1}{\sqrt{2}}F_0'\left(\frac{\omega}{2}\right)\Psi'^{(2)}\left(\frac{\omega}{2}\right),$$

$$\Psi_3'^{(4)}(\omega) = \frac{1}{\sqrt{2}}F_1'\left(\frac{\omega}{2}\right)\Psi'^{(2)}\left(\frac{\omega}{2}\right).$$

Using (13), we can then write

$$\Psi_1'^{(4)}(\omega) = j\,\text{sgn}(\omega)\,\Psi_1^{(4)}(\omega),$$

$$\Psi_2'^{(4)}(\omega) = j\,\text{sgn}(\omega)\,\frac{F_0'(\omega/2)}{F_0(\omega/2)}\Psi_2^{(4)}(\omega),$$

$$\Psi_3'^{(4)}(\omega) = j\,\text{sgn}(\omega)\,\frac{F_1'(\omega/2)}{F_1(\omega/2)}\Psi_3^{(4)}(\omega).$$

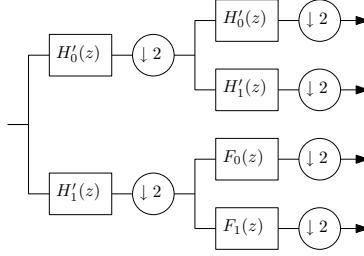Following this treatment, we conclude,

Fig. 18.   The 'dual' of the tree in Figure 16.

Theorem 1: Suppose we are given a Hilbert transform pair of wavelets $\psi(t)$, $\psi'(t)$ and a pair of CQFs $f_k(n)$, $f'_k(n)$ for $k \in \{0, 1\}$. Let $\psi_k(t)$ be the wavelets obtained by decomposing $\psi(t)$ using $f_k(n)$ for $k \in \{0, 1\}$. Also let $\psi'_k(t)$ be the wavelets obtained by decomposing $\psi'(t)$ using $f'_k(n)$ for $k \in \{0, 1\}$. Then $\psi_k(t)$ and $\psi'_k(t)$ form Hilbert transform pairs if and only if $f_k(n) = f'_k(n)$, for $k \in \{0, 1\}$.

Thus, the new wavelets form Hilbert pairs if (and only if) we set $f'_k(n) = f_k(n)$ for $k \in \{0, 1\}$. Consequently, the 'dual' of the tree in Figure 16 is obtained by simply replacing $h_k(n)$ by $h'_k(n)$ and leaving $f_k(n)$ the same, for $k \in \{0, 1\}$ (see Figure 18).

This method generates a 4-band dual-tree complex wavelet transform. The resulting scaling functions, wavelets and the spectra of the resulting complex functions are illustrated in Figure 19. For these plots, Q-shift filters [13] of length 14 are used for $h_k(n)$ and $h'_k(n)$; and $f_k(n)$ is set equal to $h_k(n)$ for $k \in \{0, 1\}$. [6]

We note that this construction is different from that given in [7]. There, the authors use the dual-tree filters to decompose the detail spaces further while here the detail spaces are decomposed further using the same filters $f_k(n)$ in each of the two trees. The method of [7] results in the complex frequency responses of certain subbands not being analytic. Also, some of the associated wavelets will not be Hilbert transform pairs, which follows from the explanations above (see Figure 20).

A. Sufficiency conditions for the M-band DT-$\mathbb{C}$WT

In [3], sufficient conditions are given for two M-band filter banks so that the associated wavelets form Hilbert transform pairs. For an M-band DT-$\mathbb{C}$WT derived from the DT-$\mathbb{C}$WPT (as described in section

---

[6] We had mentioned in Section III that there are no restrictions on $f_k(n)$. The reason for setting them equal to $h_k(n)$ here is to demonstrate that the construction in [7], which uses Q-shift filters only, can be made to yield analytic responses, by rearranging the filters.
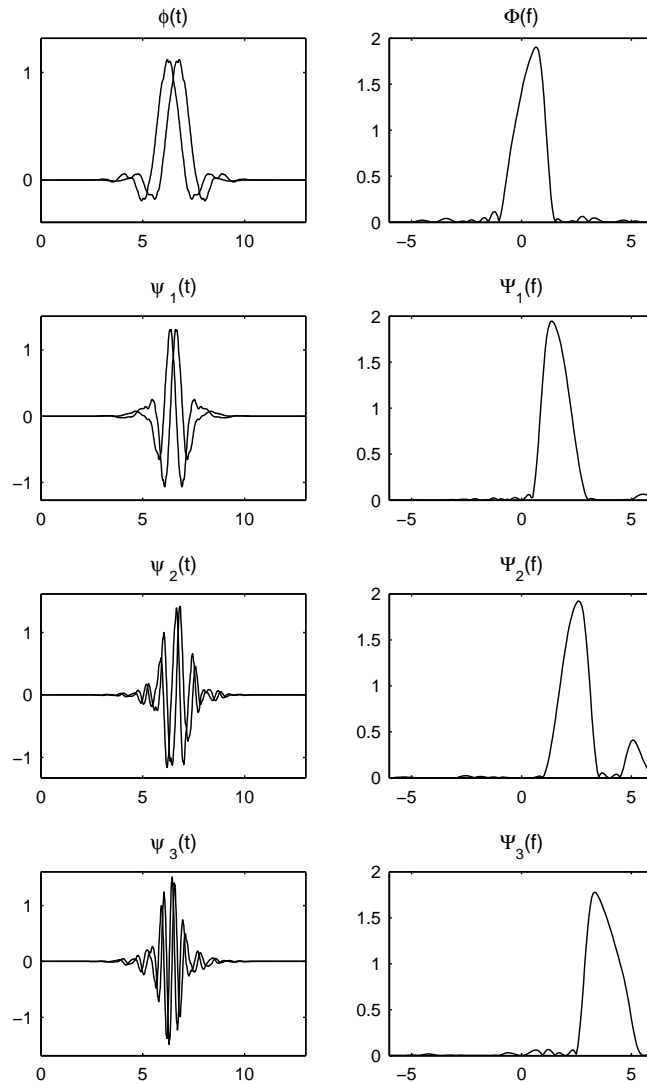
Fig. 19.   The scaling functions, wavelets and the spectra of the complex functions for the 4-band dual-tree complex wavelet transform. Note that the wavelets are approximately analytic. Q-shift filters [13] of length 14 are used to produce these figures.

IV), if one denotes the filters in the two transforms as $h_i(n)$ and $h'_i(n)$ $i \in \{0, \ldots, M-1\}$ respectively as in Figure 13; using (2), (3) and paying attention to discontinuities, it can be shown that the filters in the M-band DT-$\mathbb{C}$WT satisfy,

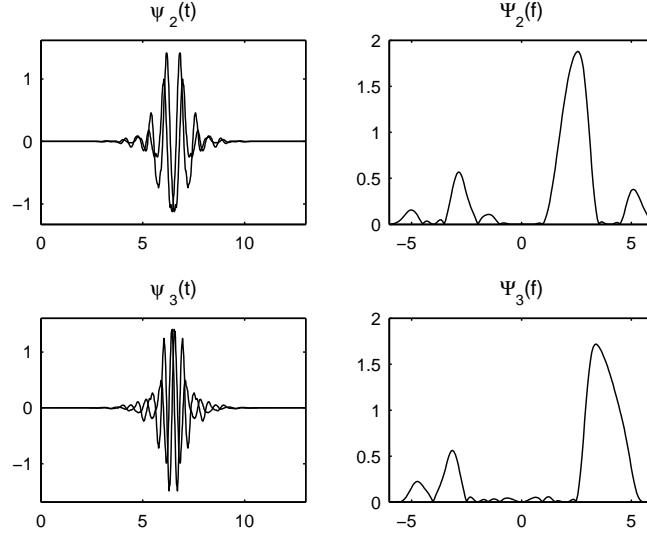$$H'_k(e^{j\omega}) = e^{-j\theta_k(\omega)} H_k(e^{j\omega})$$

Fig. 20. The wavelets $\psi_2(t)$, $\psi_3(t)$ and their spectra produced for the 4-band dual-tree complex wavelet transform produced following the description in [7]. The scaling function $\phi(t)$ and the first wavelet $\psi_1(t)$ are the same as in Figure 19, and not reproduced here. Note that the wavelets $\Psi_2(f)$, $\Psi_3(f)$ have significant energy on both positive and negative frequencies.

with

$$\theta_0(\omega) = \frac{(M-1)}{2}\omega - n\pi, \text{ for } \omega \in \left[n\frac{2\pi}{M}, (n+1)\frac{2\pi}{M}\right),$$

$$\forall n \in \left\{0, \ldots, \left\lceil\frac{M}{2}\right\rceil - 1\right\} \quad (15)$$

and

$$\theta_k(\omega) = 0.5\pi - 0.5\omega \quad \text{for } \omega \in [0, \pi), \, k \in \{1, \ldots, M-1\}. \quad (16)$$

These are exactly[7] the sufficiency conditions for Hilbert transform pairs of wavelets for the M-band case, provided in [3].

In particular, evaluating (15) and (16) for $M = 4$, we have,

$$\theta_0(\omega) = \begin{cases} 1.5\,\omega & \text{if } \omega \in [0, \pi/2) \\ 1.5\,\omega - \pi & \text{for } \omega \in [\pi/2, \pi), \end{cases} \quad (17)$$

and

$$\theta_k(\omega) = 0.5\,\pi - 0.5\,\omega \quad \text{for } \omega \in [0, \pi), \, k \in \{1, 2, 3\}. \quad (18)$$

---

[7]We assume real coefficient filters. It follows that for each k, $\theta_k(\omega)$ is an odd function on the domain $(-\pi, \pi)$. Also, for $k \neq 0$, $\theta_k(0)$ can be chosen arbitrarily since for $k \neq 0$, $H_k(e^{j0}) = 0$.
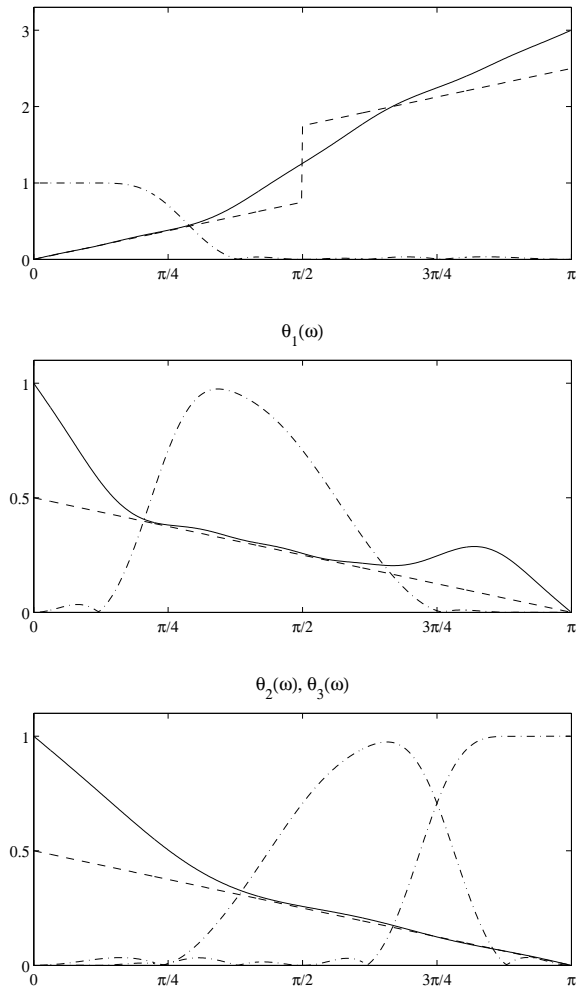
Fig. 21. Realized $\theta_k(\omega)$ (solid), desired $\theta_k(\omega)$ (dashed), and $|H_k^{(4)}(\omega)|/2$ (dash dot) for $k \in \{0, 1, 2, 3\}$. See (17), (18) for the desired $\theta_k(\omega)$.

Using FIR filters as explained, we obtained approximate $\theta_k(\omega)$ as shown in Figure 21. Note that $\theta_2(\omega) = \theta_3(\omega)$ as a consequence of our construction. For convenience, the underlying filter magnitude response is also shown. Observe that the approximations follow the ideal functions closely on the support of the underlying filter response.

B. A comparison with the general case

Despite the ease of obtaining the M-band DT-$\mathbb{C}$WT from the DT-$\mathbb{C}$WPT it should be mentioned that the transform is constrained, due to the method of construction. This can be noted by investigating the approximation and wavelet spaces. We focus on the $M = 4$ case to carry out this investigation.

In general, a 4-band DT-$\mathbb{C}$WT [2], [3] calls for approximation spaces V_i, V_i' which satisfy

$$V_i = V_{i+1} \oplus W_{i+1}^1 \oplus W_{i+1}^2 \oplus W_{i+1}^3 \tag{19}$$

and

$$V_i' = V_{i+1}' \oplus W_{i+1}'^1 \oplus W_{i+1}'^2 \oplus W_{i+1}'^3 \tag{20}$$

such that $\psi_i^k(t)$ and $\psi_i'^k(t)$ form Hilbert transform pairs for $k \in \{1, 2, 3\}$.

In contrast, our approach is based on decomposing a 2-band orthonormal wavelet basis. The approximation spaces for the 2-band basis $\hat{V}_i$, originally satisfy $\hat{V}_i = \hat{V}_{i+1} \oplus \hat{W}_{i+1}$. It is known that [14] iterating the high-pass branch as in Figure 14 corresponds to decomposing $\hat{W}_i$ as $\hat{W}_i = \hat{W}_i^0 \oplus \hat{W}_i^1$ (note that we do this only for even i). Thus, the new decomposition may be expressed as $\hat{V}_i = \hat{V}_{i+2} \oplus \hat{W}_{i+2} \oplus \hat{W}_{i+1}^0 \oplus \hat{W}_{i+1}^1$ for even i. Consequently, it can be stated that our construction employs approximation spaces V_i related to the spaces of the 2-band basis as $V_i = \hat{V}_{2i}$. This is clearly a special case of the construction in (19) and (20). Thus, it is likely that there exist superior FIR filters in terms of having shorter support for the same number of vanishing moments and providing a better approximation to Hilbert transform wavelet pairs, which may be obtained by a procedure that does not place any constraints on the structure of the 4-channel filter bank similar to the case of the real M-band DWT as in [21], [22]. However, as mentioned previously, an advantage of our construction is the ease of obtaining filters which rely on the 2-band DT-$\mathbb{C}$WT for which a body of literature is already available [9], [11], [13], [19] (also see [20] for an overview).

V. CONCLUSION

Given two DWTs that together form a DT-$\mathbb{C}$WT, we have shown how to extend each DWT so that the obtained DWPTs, forming the DT-$\mathbb{C}$WPT, possess the desirable features of the DT-$\mathbb{C}$WT, namely approximate shift-invariance and directional analysis in 2-D and higher dimensions. We proposed a basis selection algorithm to choose among the bases that the DT-$\mathbb{C}$WPT provides, by adapting the basis selection algorithm in [5]. We have also shown that, given a 2-band DT-$\mathbb{C}$WT, one can obtain an FIR implementation for the 2^b-band DT-$\mathbb{C}$WT without any need to design new filters. We have verified that the 2^b-band DT-$\mathbb{C}$WT obtained using the proposed method agrees with the conditions for the general M-band DT-$\mathbb{C}$WT given in [3].

APPENDIX A

PROOF OF LEMMA 1:

We will show (8) by induction on k. First note that for $k > 1$, we can write,

$$\frac{H'^{(k)}(e^{j\omega})}{H^{(k)}(e^{j\omega})} = \frac{H'_0(e^{j\omega})}{H_0(e^{j\omega})} \frac{H'^{(k-1)}(e^{j2\omega})}{H^{(k-1)}(e^{j2\omega})}.$$

Now suppose that,

$$\frac{H'^{(k-1)}(e^{j\omega})}{H^{(k-1)}(e^{j\omega})} = -j\,\mathrm{sgn}(\omega)e^{j0.5\omega} \quad \text{for } |\omega| < \pi.$$

It can then be verified that (taking into account the periodicity by 2π),

$$\frac{H'^{(k-1)}(e^{j2\omega})}{H^{(k-1)}(e^{j2\omega})} = -j\,\mathrm{sgn}(\omega)e^{j\omega} \quad \text{for } |\omega| < \pi. \tag{21}$$

Multiplying this by

$$\frac{H'_0(e^{j\omega})}{H_0(e^{j\omega})} = e^{-j0.5\omega} \quad \text{for } |\omega| < \pi,$$

we see that the desired relationship holds for the kth stage if it holds for the $(k-1)^{\text{th}}$ stage. By our definition of $H^{(1)}$ and $H'^{(1)}$ in (5) and (6), it follows by induction that (8) is true.

APPENDIX B

PROOF OF COROLLARY 1:

Using (4), we have for $k > 1$

$$H_{\text{new}}^{(k)}(e^{j\omega}) = \frac{H_0^{(1)}(e^{j\omega})}{H_0(e^{j\omega})} H^{(k)}(e^{j\omega}) \quad \text{for } |\omega| < \pi \tag{22}$$

and

$$H_{\text{new}}'^{(k)}(e^{j\omega}) = \frac{H_0'^{(1)}(e^{j\omega})}{e^{-j0.5\omega}H_0(e^{j\omega})} H'^{(k)}(e^{j\omega}) \quad \text{for } |\omega| < \pi. \tag{23}$$

Now, using (7), (22), (23), we can write for $k > 1$,

$$H_{\text{new}}'^{(k)}(e^{j\omega}) = -j\,\mathrm{sgn}(\omega)\,e^{j\omega}\,\frac{H_0'^{(1)}(e^{j\omega})}{H_0^{(1)}(e^{j\omega})}\,H_{\text{new}}^{(k)}(e^{j\omega})$$

$$\text{for } |\omega| < \pi.$$

Therefore, for $k > 1$,

$$H_{\text{new}}'^{(k)}(e^{j\omega}) = -j\,\mathrm{sgn}(\omega)\,H_{\text{new}}^{(k)}(e^{j\omega})$$

$$= -\mathcal{H}\left\{H_{\text{new}}^{(k)}(e^{j\omega})\right\},$$

(notice that this is equivalent to (9)) if and only if,

$$H_0'^{(1)}(e^{j\omega}) = e^{-j\omega} H_0^{(1)}(e^{j\omega}),$$

which is equivalent to (10).

REFERENCES

[1] İ. Bayram and I. W. Selesnick. A simple construction for the M-band dual-tree complex wavelet transform. In *Proc. 12th IEEE DSP Workshop*, 2006.

[2] C. Chaux, L. Duval, and J.-C. Pesquet. Hilbert pairs of M-band orthonormal wavelet bases. In *Proc. Eur. Sig. and Image Proc. Conf.*, 2004.

[3] C. Chaux, L. Duval, and J.-C. Pesquet. Image analysis using a dual-tree M-band wavelet transform. *IEEE Trans. Image Processing*, 15(8):2397–2412, August 2006.

[4] I. Cohen, S. Raz, and D. Malah. Orthonormal shift-invariant wavelet packet decomposition and representation. *Signal Processing*, 57(3):251–270, January 1997.

[5] R. R. Coifman and M. V. Wickerhauser. Entropy-based algorithms for best basis selection. *IEEE Trans. Information Theory*, 38(2):713–718, March 1992.

[6] A. Jalobeanu, L. Blanc-Féraud, and J. Zerubia. Satellite image deconvolution using complex wavelet packets. In *Proc. IEEE Int. Conf. on Image Processing (ICIP)*, 2000.

[7] A. Jalobeanu, L. Blanc-Féraud, and J. Zerubia. Satellite image deblurring using complex wavelet packets. *International Journal of Computer Vision*, 51(3):205–217, 2003.

[8] A. Jalobeanu, N. Kingsbury, and J. Zerubia. Image deconvolution using hidden Markov tree modeling of complex wavelet packets. In *Proc. IEEE Int. Conf. on Image Processing (ICIP)*, 2001.

[9] N. G. Kingsbury. The dual-tree complex wavelet transform: A new efficient tool for image restoration and enhancement. In *Proc. Eur. Sig. Proc. Conf (EUSIPCO)*, 1998.

[10] N. G. Kingsbury. Image processing with complex wavelets. *Philos. Trans. R. Soc. London A, Math. Phys. Sci.*, 357(1760):2543–2560, September 1999.

[11] N. G. Kingsbury. A dual-tree complex wavelet transform with improved orthogonality and symmetry properties. In *Proc. IEEE Int. Conf. on Image Processing (ICIP)*, 2000.

[12] N. G. Kingsbury. Complex wavelets for shift invariant analysis and filtering of signals. *J. of Appl. and Comp. Harm. Analysis*, 10(3):234–253, May 2001.

[13] N. G. Kingsbury. Design of Q-shift complex wavelets for image processing using frequency domain energy minimization. In *Proc. IEEE Int. Conf. on Image Processing (ICIP)*, 2003.

[14] S. Mallat. *A Wavelet Tour of Signal Processing*. Academic Press, 1998.

[15] A. V. Oppenheim, R. W. Schafer, and J. R. Buck. *Discrete-Time Signal Processing*. Prentice-Hall, 1999.

[16] H. Ozkaramanli and R. Yu. On the phase condition and its solution for Hilbert transform pairs of wavelet bases. *IEEE Trans. Signal Processing*, 51(12):3293–3294, December 2003.

[17] K. Ramchandran and M. Vetterli. Best wavelet packet basis in a rate-distortion sense. *IEEE Trans. Image Processing*, 2(2):160–175, April 1993.

[18] I. W. Selesnick. Hilbert transform pairs of wavelet bases. *IEEE Signal Processing Letters*, 8(6):170–173, June 2001.

[19] I. W. Selesnick. The design of approximate Hilbert transform pairs of wavelet bases. *IEEE Trans. Signal Processing*, 50(5):1144–1152, May 2002.

[20] I. W. Selesnick, R. G. Baraniuk, and N. G. Kingsbury. The dual-tree complex wavelet transform - A coherent framework for multiscale signal and image processing. *IEEE Signal Processing Magazine*, 22(6):123–151, November 2005.

[21] P. Steffen, P. N. Heller, R. A. Gopinath, and C. S. Burrus. Theory of regular M-band wavelet bases. *IEEE Trans. Signal Processing*, 41(12):3497–3511, December 1993.

[22] G. V. Welland and M. Lundberg. Construction of compact p-wavelets. *Constructive approximation*, 9(2-3):347–370, June 1993.

[23] M. V. Wickerhauser. *Adapted Wavelet Analysis from Theory to Software*. AK Peters, Ltd., 1994.

[24] Z. Xie, E. Wang, G. Zhang, G. Zhao, and X. Chen. Seismic signal analysis based on the dual-tree complex wavelet packet transform. *Acta Seismologica Sinica*, 17(1):117–122, November 2004.

[25] R. Yu and H. Ozkaramanli. Hilbert transform pairs of orthogonal wavelet bases: Necessary and sufficient conditions. *IEEE Trans. Signal Processing*, 53(12):4723–4725, December 2005.